Time-delay interferometry for LISA

Massimo Tinto,* F. B. Estabrook,† and J. W. Armstrong‡
Jet Propulsion Laboratory, California Institute of Technology Pasadena, California 91109

(Received 17 August 2001; published 2 April 2002)

LISA (Laser Interferometer Space Antenna) is a mission to detect and study low-frequency cosmic gravitational radiation through its influence on the phases or frequencies of laser beams exchanged between three remote spacecraft. We previously showed how, with lasers of identical frequencies on stationary spacecraft, the measurement of twelve time series of Doppler shifts could be combined to cancel exactly the phase noise of the lasers and the Doppler fluctuations due to noninertial motions of the six optical benches, while preserving gravitational wave signals. Here we generalize those results on gravitational wave detection with time-delay interferometry to the expected LISA instrument. The six lasers have different center frequencies (in the nominal LISA configuration these center frequencies may well differ by several hundred megahertz) and the distances between spacecraft pairs will change with time (these slowly varying orbital Doppler shifts are expected to be up to tens of megahertz). We develop time-delay data combinations which, as previously, preserve gravitational waves and exactly cancel the leading noise source (phase fluctuations of the six lasers); these data combinations then imply transfer functions for the remaining system noises. Using these, we plot frequency and phase power spectra for modeled system noises in the unequal Michelson combination X and the symmetric Sagnac combination ζ. Although optical bench noise can no longer be cancelled exactly, with the current LISA specifications it is suppressed to negligible levels. It is known that the presently anticipated laser center frequency differences and the orbital Doppler drifts introduce another source of phase noise, arising from the onboard oscillators required to track the photodetector fringes. For the presently planned mission, our analysis indeed demonstrates that noise from current-generation ultrastable oscillators would, if uncorrected, dominate the LISA noise budget. To meet the LISA sensitivity goals either achievable improvements in oscillator stability must be combined with much stricter requirements on the allowed laser center frequency differences and on the allowed Doppler shifts from orbital drifts or, as has been previously suggested, additional calibrating interspacecraft data must be taken, by modulating the laser beams and considerably increasing system complexity. We generalize prior schemes for obtaining the required oscillator instability calibration data to the case of six proof masses, six lasers, and three onboard oscillators. For this realistic configuration we derive appropriate time-delayed combinations of the calibrating data to correct each of the laser-noise-free data combinations.

DOI: 10.1103/PhysRevD.65.082003 PACS number(s): 04.80.Nn, 07.60.Ly, 95.55.Ym

I. INTRODUCTION

LISA (Laser Interferometer Space Antenna) is a three-spacecraft deep space mission, jointly proposed to the National Aeronautics and Space Administration (NASA) and the European Space Agency (ESA). It will detect and study low-frequency cosmic gravitational radiation by observing frequency shifts of laser beams interchanged between drag-free spacecraft [1].

Modeling each spacecraft with two optical benches, carrying independent lasers, beam splitters, and photodetectors, we previously analyzed the measured twelve time series of frequency shifts (six one-way laser beams between spacecraft pairs, and six more between the two optical benches on each of the three spacecraft). We showed that there exist several combinations of these twelve observables that exactly cancel both the otherwise overwhelming phase noise of the lasers, and the phase fluctuations due to the noninertial motions of the six optical benches, while leaving effects due to passing gravitational waves [2–4].

The analyses in our previous work, however, relied on the assumptions that (i) the spacecraft were stationary relative to each other (but also in free fall, drag free) and (ii) the intrinsic (or center) frequencies of the six lasers were all equal. Here we amend and extend those results to the realistic LISA operational configuration, in which the center frequencies of the lasers may well all differ by several hundred megahertz, and the spacecraft are drifting in their flight formation, resulting in slowly varying Doppler shifts of tens of megahertz [5].

As a consequence of having lasers with different frequencies, the phase noise due to the vibrations of the optical benches will no longer cancel out exactly in the laser-noise-free data combinations, and optical bench motion spectral density must now be modeled and kept below the design threshold. Perhaps more serious is that both frequency offsets between lasers and Doppler drifts now bring in another source of phase noise, arising in the onboard clocks or oscillators [ultra stable oscillators (USOs)] used in the frequency down conversion and tracking of photodetector fringe rates. In this paper we address the general problem of removing these noises from all the laser-noise-free combinations previously derived.

*Electronic address: Massimo.Tinto@jpl.nasa.gov
†Electronic address: Frank.B.Estabrook@jpl.nasa.gov
‡Electronic address: John.W.Armstrong@jpl.nasa.gov

In Sec. II we model the raw data: twelve one-way measurements of phase differences at the photodetectors. These require base banding (or down conversion) with locally generated frequencies to compensate for laser-frequency offsets and Doppler shifts from spacecraft motions. As a consequence, now the twelve phase measurement models include terms involving the noises of the oscillators (USOs) driving the heterodyne measurements. To facilitate comparison with previous results in Refs. [1,6,7], here we give the equations for data in terms of measured phases. To facilitate comparison with the notation of our previous papers [2–4], we also include a summary in the Appendix where the data is equivalently expressed in terms of measured frequencies.

In Sec. III we derive the laser-noise-free unequal-arm-interferometric combination we call X_q, the combination α_q, and the totally symmetric Sagnac combination ζ_q. Equivalent combinations of frequency data, denoted with the same symbols, are described in the Appendix. These combinations correspond to those derived in Ref. [4], but now they include the effects of lasers with different frequencies, spacecraft moving relative to each other, and USO noises. For each combination, transfer functions are implied for the remaining system noises arising from optical bench motion, optical path fluctuations (shot noise), proof mass buffeting (acceleration noise), and now USO phase noise. We give plots of both frequency and phase system noise spectra that will appear in the combinations X_q and ζ_q. We discuss requirements on USO noise so that the desired sensitivity to gravitational radiation can be achieved. If intrinsic oscillator phase noise cannot be reduced to this level, with improved USOs, and by placing system requirements on laser frequency offsets and orbital drifts, it will be necessary to take additional data for calibration, which we consider in Sec. IV. Bender *et al.* [1] have proposed modulation of the laser beams with USO generated frequencies. Hellings *et al.* [6], and Hellings [7] have analyzed a two-frequency version, for the case when bench noises were not included, and only one laser in each spacecraft was assumed. We derive generalized expressions for combinations of six streams of calibrating data, which can be used for removing the USO noises from all the previously identified laser-noise-free combinations. These calibration data are different from those previously published [7] in that they also take account of the USO noise introduced in the down conversion of the phase measurements between each pair of optical benches within each spacecraft. In Sec. V we discuss the sensitivities of the newly derived interferometric combinations and present our concluding remarks.

II. TIME-DELAY INTERFEROMETRY

In what follows we present the principle of time-delay interferometry discussed in Ref. [4] (which we will refer to as paper I), now in terms of relative phase rather than frequency measurements. This is because the analysis becomes somewhat simpler by working with phase rather than frequency when the six lasers have offset frequencies, and when the spacecraft have relative velocities; a direct comparison with Refs. [6,7] is also easier. For completeness we provide in the Appendix equations for data entering the corresponding time-delay interferometric combinations of frequency measurements and a glossary of notations from our previous papers.

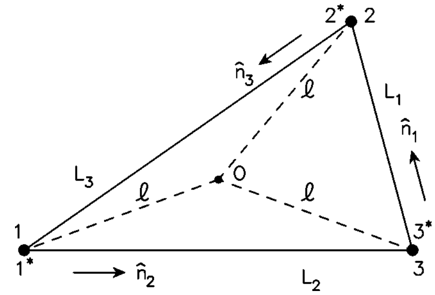

FIG. 1. Schematic LISA configuration. The three spacecraft are equidistant from point o in the plane of the spacecraft. Unit vectors $\hat{n}_i$ point between spacecraft pairs with the indicated orientations. L_i are the (unequal) arm lengths; at each spacecraft there are two optical benches (denoted 1, 1^*, etc.), as indicated.

Figure 1 shows the overall geometry of the LISA detector. The spacecraft are labeled 1, 2, 3 and distances between pairs of spacecraft are L_1, L_2, L_3, with L_i being opposite spacecraft *i*. Unit vectors between spacecraft are $\hat{n}_i$, oriented as indicated in Fig. 1. We similarly index the phase difference data to be analyzed: s_{31} is the phase difference time series measured at reception at spacecraft 1 with transmission from spacecraft 2 (along L_3). This slightly odd convention should be carefully noted. It is perhaps unfortunate, as denoting it as "s_{21}" might seem more immediate. Our convention was adopted in Ref. [3], and we have adhered to it so that all papers in the series can be intercompared more easily. Similarly, s_{21} is the phase difference series derived from reception at spacecraft 1 with transmission from spacecraft 3. The other four one-way phase difference time series from signals exchanged between the spacecraft are obtained by cyclic permutation of the indices $1\rightarrow 2\rightarrow 3\rightarrow 1$. We also use a useful notation for delayed data streams: $s_{31,2}=s_{31}(t-L_2)$, $s_{31,23}=s_{31}(t-L_2-L_3)=s_{31,32}$, etc. (we take the speed of light $c=1$ for the analysis). Six more phase difference series result from laser beams exchanged between adjacent optical benches within each spacecraft; these are similarly indexed as τ_{ij} $(i,j=1,2,3; i\neq j)$.

The proof-mass-plus-optical-bench assemblies for LISA spacecraft number 1 are shown schematically in Fig. 2. We take the left-hand optical bench to be bench number 1, while the right-hand bench is 1^*. The photo detectors that generate the data s_{21}, s_{31}, τ_{21}, and τ_{31} at spacecraft 1 are shown. The phase fluctuation of the laser on optical bench 1 is $p_1(t)$; on optical bench 1^* it is $p_1^*(t)$ and these are independent (the lasers are not "locked"). We extend the cyclic terminology that at vertex i $(i=1,2,3)$ the random displacement vectors of the two proof masses are, respectively, denoted $\vec{\delta}_i(t)$ and $\vec{\delta}_i^*(t)$, and the random displacements (perhaps several orders of magnitude greater) of their optical benches are correspondingly denoted $\vec{\Delta}_i(t)$ and $\vec{\Delta}_i^*(t)$. As we pointed out in paper I, our analysis does *not* assume that pairs of optical benches are rigidly connected, i.e., $\vec{\Delta}_i \neq \vec{\Delta}_i^*$, in general. The

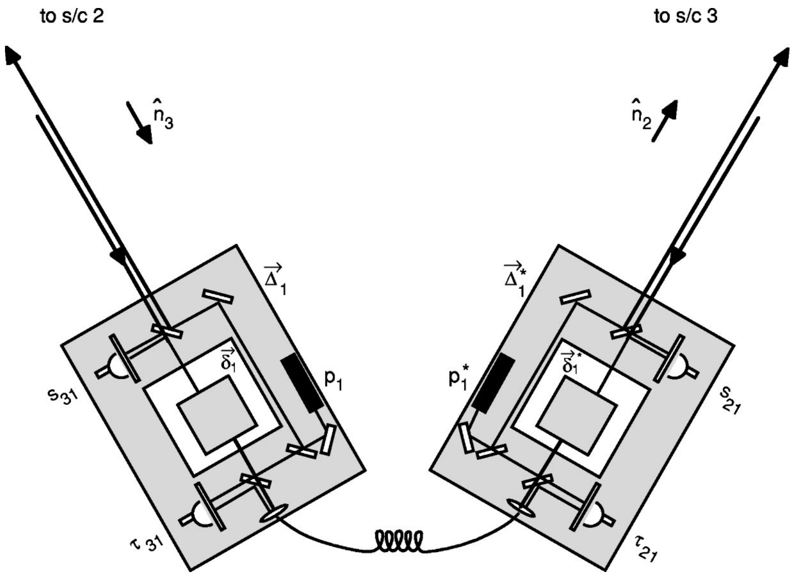

FIG. 2. Schematic diagram, adapted from Ref. [12], of the proof-mass and optical bench assemblies for LISA spacecraft 1. The left bench reads out a phase signal s_{31} (from spacecraft 2, bounced off the left proof mass, read out using the laser and the photodetector on the left optical bench) and τ_{31} (from the right optical bench, bounced off the back of the right proof mass, directed through the optical fiber and read out using the laser photodetector on the left bench). The right bench analogously reads out s_{21} and τ_{21}. The random displacements of the proof masses and optical benches are indicated with $\vec{\delta}_i$ for the proof masses, and with $\vec{\Delta}_i$ $(i=1,2,3)$ for the optical benches.

present LISA design shows optical fibers transmitting signals both ways between adjacent benches. We ignore time-delay effects for these signals and will simply denote by $\mu_i(t)$ the phase fluctuations upon transmission through the fibers of the laser beams with frequencies ν_i and ν_i^*. The $\mu_i(t)$ phase shifts within a given spacecraft might not be the same for large frequency differences $\nu_i-\nu_i^*$. For the envisioned frequency differences (a few hundred megahertz), however, the remaining fluctuations due to the optical fiber can be neglected [8].

Figure 2 endeavors to make the detailed light paths for these observations clear. An outgoing light beam transmitted to a distant spacecraft is routed from the laser on the local optical bench using mirrors and beam splitters; this beam does not interact with the local proof mass. Conversely, an *incoming* light beam from a distant spacecraft is bounced off the local proof mass before being reflected onto the photodetector where it is mixed with light from the laser on that same optical bench. Since the relative velocities $\dot{L}_i(t)$ between a pair of spacecraft will induce several megahertz Doppler on the received frequency of the laser light [5], and furthermore the frequencies of the lasers themselves can be different by several hundred megahertz [1], the outputs of the photodetectors have a large fringe rate, or "beat-note" frequency, and must be properly down converted—tracked—before measurements of phase fluctuations in the gravitational wave band are made. In order to perform this down conversion, each spacecraft is provided with an onboard clock, which is called the ultrastable oscillator (USO), to generate the tracking (or base-banding) frequency. We will characterize each USO with a frequency f_i, which brings along phase fluctuations q_i at that frequency $(i=1,2,3)$, and as in Ref. [6] we introduce multipliers to generate the required tracking frequencies (we suggest phase-lock loops for this frequency tracking in Sec. IV). The interspacecraft phase data are denoted s_{31} and s_{21} in Fig. 2.

Beams between adjacent optical benches within a single spacecraft are bounced off proof masses in the opposite way. Light to be *transmitted* from the laser on an optical bench is *first* bounced off the proof mass it encloses and then directed to the other optical bench. Upon reception it does *not* interact with the proof mass there, but is directly mixed with local laser light, and again down converted. These data are denoted τ_{31} and τ_{21} in Fig. 2.

The terms in the following equations for the s_{ij} and τ_{ij} phase measurements can now be developed from Figs. 1 and 2. Consider the $s_{31}(t)$ process [Eq. (3)] below. The photodetector on the left bench of spacecraft 1, which (in the spacecraft frame) experiences a time-varying displacement $\vec{\Delta}_1$, measures the phase difference s_{31} by first mixing the beam of frequency ν_2^* from the distant optical bench 2^* in direction $\hat{n}_3$ [which has slowly varying Doppler shift $(1-\dot{L}_3)$, and laser phase noise p_2^* and optical bench motion $\vec{\Delta}_2^*$ that have been delayed by propagation along L_3], after one bounce off the proof mass $(\vec{\delta}_1)$, with the local laser light (of frequency ν_1 with phase noise p_1), and then down converting the difference with the local frequency $a_{31}f_1$ to remove the large (but slowly varying) frequency offset. In Eq. (4) the τ_{31} measurement results from light originating at the right-bench laser $(\nu_1^*, p_1^*, \vec{\Delta}_1^*)$, bounced once off the right proof mass $(\vec{\delta}_1^*)$, and directed through the fiber [incurring phase shift $\mu_1(t)$], to the left bench, where it is mixed with laser light (ν_1, p_1), and again down converted. Similarly the right bench records the phase differences s_{21} and τ_{21}. The four data streams recorded at vertex 1, including Doppler effects, lasers with different frequencies, gravitational wave signals, optical path noises, proof-mass and bench noises, and USO phase fluctuations, are now given by the following expressions:

$$\begin{aligned} s_{21}=&[\nu_3(1-\dot{L}_2)-\nu_1^*-a_{21}f_1]t+p_{3,2}-p_1^*-a_{21}q_1\\ &-\nu_3\hat{n}_2\cdot\vec{\Delta}_{3,2}+\nu_3(1-\dot{L}_2)[2\hat{n}_2\cdot\vec{\delta}_1^*-\hat{n}_2\cdot\vec{\Delta}_1^*]\\ &+s_{21}^{\rm gw}+s_{21}^{\rm opt.\ path}, \end{aligned} \tag{1}$$

$$\tau_{21}=[\nu_1-\nu_1^*-c_{21}f_1]t+p_1-p_1^*-c_{21}q_1 + 2\nu_1\hat{n}_3\cdot(\vec{\delta}_1-\vec{\Delta}_1)+\mu_1, \tag{2}$$

$$s_{31}=[\nu_2^*(1-\dot{L}_3)-\nu_1-a_{31}f_1]t+p_{2,3}^*-p_1-a_{31}q_1 + \nu_2^*\hat{n}_3\cdot\vec{\Delta}_{2,3}^*+\nu_2^*(1-\dot{L}_3)[-2\hat{n}_3\cdot\vec{\delta}_1+\hat{n}_3\cdot\vec{\Delta}_1] + s_{31}^{\text{gw}}+s_{31}^{\text{opt. path}}, \tag{3}$$

$$\tau_{31}=[\nu_1^*-\nu_1-c_{31}f_1]t+p_1^*-p_1-c_{31}q_1 - 2\nu_1^*\hat{n}_2\cdot(\vec{\delta}_1^*-\vec{\Delta}_1^*)+\mu_1. \tag{4}$$

For all the down conversions at spacecraft 1, the USO-generated frequency f_1 is used, and the coefficients a_{21}, a_{31}, c_{21}, and c_{31} we envision as estimated via phase-lock loops driving numerically controlled oscillators, to remove the large frequency offsets in the phase measurements (the ‘‘beat notes’’) [6,7]. This is shown in Fig. 5. Thus the values of these coefficients are determined by the following expressions:

$$a_{21}=\frac{\nu_3(1-\dot{L}_2)-\nu_1^*}{f_1}, \tag{5}$$

$$a_{31}=\frac{\nu_2^*(1-\dot{L}_3)-\nu_1}{f_1}, \tag{6}$$

$$c_{31}=-c_{21}=\frac{\nu_1^*-\nu_1}{f_1}. \tag{7}$$

Eight other relations, for the readouts at vertices 2 and 3, are given by cyclic permutation of the indices in Eqs. (1)–(7).

The gravitational wave phase signal components in Eqs. (1) and (3) are given by integrating with respect to time the Eqs. (1), (2) of Ref. [3] that related frequency shifts to metric perturbations. The optical path phase noise contributions $s_{ij}^{\text{opt. path}}$ due mainly to shot noise from the low signal-to-noise ratio (SNR) in the links connecting the distant spacecraft, can be derived from the corresponding term given in Ref. [4]. The τ_{ij} measurements will be made with high SNR so that for them the shot noise is negligible.

The expressions of the phase measurements given by Eqs. (1)–(4) imply (as will be evident below) that if we would substitute them into the laser-noise-free combinations derived in paper I, the resulting data would now be affected by bench noise, and most importantly by the USO phase fluctuations, which have been denoted q_i $(i=1,2,3)$. For instance, with a state-of-the-art USO displaying a frequency stability of about 1.0×10^{-13} in the millihertz frequency band, the corresponding relative frequency fluctuations $\dot{q}_i/\nu_i$ introduced by the USO in the laser-noise-free data combinations would be equal to about 3.0×10^{-20}, several orders of magnitude above the LISA sensitivity goals [1]. In what follows we will address the USO noise, and we will identify the magnitude of the remaining bench noise in the USO-corrected data combinations.

III. INTERFEROMETRIC COMBINATIONS FOR LISA

The laser-noise-free combinations of phase data can readily be obtained from those given in paper I for frequency data. We use the same notations: X, Y, Z, α, β, γ, ζ, etc., but with a subscript q to emphasize that as yet no USO calibrating data has been incorporated.

The drag-free LISA unequal-arm-length interferometric combination, which we denote here with X_q, is now[1] [4]

$$X_q=s_{32,322}-s_{23,233}+s_{31,22}-s_{21,33}+s_{23,2}-s_{32,3}+s_{21}-s_{31} + \frac{1}{2}(-\tau_{21,2233}+\tau_{21,33}+\tau_{21,22}-\tau_{21})+\frac{1}{2}(+\tau_{31,2233} - \tau_{31,33}-\tau_{31,22}+\tau_{31}). \tag{8}$$

After substituting the phase differences s_{ij}, τ_{ij} given by Eqs. (1)–(4) into Eq. (8), all terms p_i, p_i^* are eliminated. We derive the following expression for X_q, reflecting contributions from gravitational wave, optical path noise, USO noise, proof mass noise, and optical bench noise:

$$\begin{aligned}X_q={}&X^{\text{gw}}+X^{\text{opt. path}}+a_{32}[q_{2,3}-q_{2,322}]-a_{23}[q_{3,2}-q_{3,233}]+a_{31}[q_1-q_{1,22}]-a_{21}[q_1-q_{1,33}]+c_{21}[(q_1-q_{1,22})-(q_1\\&-q_{1,22})_{,33}]-\nu_1^*\hat{n}_2\cdot\vec{\delta}_{1,2233}^*-\nu_1\hat{n}_3\cdot\vec{\delta}_{1,2233}+2\nu_1(1-\dot{L}_3)\hat{n}_3\cdot\vec{\delta}_{2,322}^*+2\nu_1^*(1-\dot{L}_2)\hat{n}_2\cdot\vec{\delta}_{3,233}+[\nu_1-2\nu_2^*(1-\dot{L}_3)]\hat{n}_3\cdot\vec{\delta}_{1,22}\\&+[\nu_1^*-2\nu_3(1-\dot{L}_2)]\hat{n}_2\cdot\vec{\delta}_{1,33}^*+\nu_1^*\hat{n}_2\cdot\vec{\delta}_{1,22}^*+\nu_1\hat{n}_3\cdot\vec{\delta}_{1,33}-2\nu_1^*(1-\dot{L}_2)\hat{n}_2\cdot\vec{\delta}_{3,2}-2\nu_1(1-\dot{L}_3)\hat{n}_3\cdot\vec{\delta}_{2,3}^*+[2\nu_3(1-\dot{L}_2)\\&-\nu_1^*]\hat{n}_2\cdot\vec{\delta}_1^*+[2\nu_2^*(1-\dot{L}_3)-\nu_1]\hat{n}_3\cdot\vec{\delta}_1+[\nu_2^*-\nu_1(1-\dot{L}_3)]\hat{n}_3\cdot[\vec{\Delta}_{2,322}^*-\vec{\Delta}_{2,3}^*]+[\nu_3-\nu_1^*(1-\dot{L}_2)]\hat{n}_2\cdot[\vec{\Delta}_{3,233}-\vec{\Delta}_{3,2}]\\&+[\nu_1-\nu_2^*(1-\dot{L}_3)]\hat{n}_3\cdot[\vec{\Delta}_1-\vec{\Delta}_{1,22}]+[\nu_1^*-\nu_3(1-\dot{L}_2)]\hat{n}_2\cdot[\vec{\Delta}_1^*-\vec{\Delta}_{1,33}^*],\end{aligned} \tag{9}$$

[1]In order for this and other interferometric combinations to be effective, the arm lengths need to be known to the experimenters within a well specified accuracy [2]. The arm length accuracy depends on the magnitude of the lasers phase stability and the level of the secondary noise sources, and was derived by requiring the phase noise due to the lasers remaining in the interferometric combinations to be smaller than the phase fluctuations arising from secondary noise sources. For nominal LISA parameters [1,2] and the Michelson combination X, the arm lengths must be known to about 30 m to cancel laser phase noise to the level of photon counting statistics.

where we have denoted with X^{gw} and $X^{\text{opt. path}}$ the contributions of the gravitational wave signal and the optical path fluctuations to the unequal-arm interferometric phase response.

It should first be noticed that, with laser frequency offsets of the order of a few hundred megahertz, the magnitude of the proof-mass noise terms $\vec{\delta}_i$ and $\vec{\delta}_i^*$ entering in X_q will be essentially equal to that discussed in paper I. This is because changes in their coefficients in X_q will be of order 10^{-6} (typical difference between two lasers frequencies divided by the nominal frequency of the lasers). The magnitude of the remaining bench noise, however [given in Eq. (9) by the $\vec{\Delta}_i$, $\vec{\Delta}_i^*$ terms], needs to be estimated. If we assume the optical bench noise to be equal to 10 nm/$\sqrt{\mathrm{Hz}}$ [11], Eq. (9) implies that the corresponding relative frequency (strain) fluctuations remaining in X_q are equal to about $10^{-24}/\sqrt{\mathrm{Hz}}$ at 10^{-3} Hz, a negligible contribution to the unequal-arm response strain noise budget.

Three other independent laser-noise-free linear combinations of the phase difference measurements are defined by the following expression and its cyclic permutations [4]:

$$\alpha_q = s_{21} - s_{31} + s_{13,2} - s_{12,3} + s_{32,12} - s_{23,13} - \frac{1}{2}(\tau_{13,2} + \tau_{13,13} + \tau_{21} + \tau_{21,123} + \tau_{32,3} + \tau_{32,12}) + \frac{1}{2}(\tau_{23,2} + \tau_{23,13} + \tau_{31} + \tau_{31,123} + \tau_{12,3} + \tau_{12,12}), \tag{10}$$

where we have denoted with α_q the interferometric combination uncalibrated for the USO phase fluctuations. After substituting the phase difference data s_{ij}, τ_{ij} given by Eqs. (1)–(4) into Eq. (10), we find

$$\begin{aligned}\alpha_q = {} & \alpha^{\mathrm{gw}} + \alpha^{\text{opt. path}} + [a_{31} - a_{21}]q_1 + c_{21}[q_1 + q_{1,123}] + [c_{32} + a_{12}]q_{2,3} + [c_{13} - a_{13}]q_{3,2} + [c_{32} - a_{32}]q_{2,12} + [c_{13} + a_{23}]q_{3,13} \\ & + [2\nu_2^*(1-\dot{L}_3) - \nu_1]\hat{n}_3 \cdot \vec{\delta}_1 + [2\nu_3(1-\dot{L}_2) - \nu_1^*]\hat{n}_2 \cdot \vec{\delta}_1^* + [2\nu_2(1-\dot{L}_1) - \nu_3^*]\hat{n}_1 \cdot \vec{\delta}_{3,2}^* + [2\nu_3^*(1-\dot{L}_1) - \nu_2]\hat{n}_1 \cdot \vec{\delta}_{2,3} \\ & + [2\nu_1(1-\dot{L}_3) - \nu_2^*]\hat{n}_3 \cdot \vec{\delta}_{2,12}^* + [2\nu_1^*(1-\dot{L}_2) - \nu_3]\hat{n}_2 \cdot \vec{\delta}_{3,13} - \nu_3 \hat{n}_2 \cdot \vec{\delta}_{3,2} - \nu_3^* \hat{n}_1 \cdot \vec{\delta}_{3,13}^* - \nu_1^* \hat{n}_2 \cdot \vec{\delta}_{1,123}^* - \nu_1 \hat{n}_3 \cdot \vec{\delta}_{1,123} \\ & - \nu_2^* \hat{n}_3 \cdot \vec{\delta}_{2,3}^* - \nu_2 \hat{n}_1 \cdot \vec{\delta}_{2,12} + [\nu_2^* - \nu_1(1-\dot{L}_3)]\hat{n}_3 \cdot \vec{\Delta}_{2,12}^* + [\nu_3 - \nu_1^*(1-\dot{L}_2)]\hat{n}_2 \cdot \vec{\Delta}_{3,13} + [\nu_3^* - \nu_2(1-\dot{L}_1)]\hat{n}_1 \cdot \vec{\Delta}_{3,2}^* \\ & + [\nu_2 - \nu_3^*(1-\dot{L}_1)]\hat{n}_1 \cdot \vec{\Delta}_{2,3} + [\nu_1 - \nu_2^*(1-\dot{L}_3)]\hat{n}_3 \cdot \vec{\Delta}_1 + [\nu_1^* - \nu_3(1-\dot{L}_2)]\hat{n}_2 \cdot \vec{\Delta}_1^* . \end{aligned} \tag{11}$$

A symmetric data combination which exactly cancels all laser noises and has the property that each of the s_{ij} enters exactly once and is lagged by exactly one of the one-way light times is ζ_q [4]. Its expression in terms of the one-way phase measurements is equal to

$$\zeta_q = s_{32,2} - s_{23,3} + s_{13,3} - s_{31,1} + s_{21,1} - s_{12,2} + \frac{1}{2}(-\tau_{13,21} + \tau_{23,12} - \tau_{21,23} + \tau_{31,23} - \tau_{32,13} + \tau_{12,13}) + \frac{1}{2}(-\tau_{32,2} + \tau_{12,2} - \tau_{13,3} + \tau_{23,3} - \tau_{21,1} + \tau_{31,1}). \tag{12}$$

After substituting the phase difference data s_{ij}, τ_{ij} given by Eqs. (1)–(4) into Eq. (12), we find

$$\begin{aligned}\zeta_q = {} & \zeta^{\mathrm{gw}} + \zeta^{\text{opt. path}} + [a_{31} - a_{21} + c_{21}]q_{1,1} + [a_{12} - a_{32} + c_{32}]q_{2,2} + [a_{23} - a_{13} + c_{13}]q_{3,3} + c_{21}q_{1,23} + c_{32}q_{2,31} + c_{13}q_{3,12} - \nu_1 \hat{n}_3 \cdot \vec{\delta}_{1,23} \\ & - \nu_1^* \hat{n}_2 \cdot \vec{\delta}_{1,23}^* - \nu_2 \hat{n}_1 \cdot \vec{\delta}_{2,13} - \nu_2^* \hat{n}_3 \cdot \vec{\delta}_{2,13}^* - \nu_3 \hat{n}_2 \cdot \vec{\delta}_{3,12} - \nu_3^* \hat{n}_1 \cdot \vec{\delta}_{3,12}^* + [2\nu_2^*(1-\dot{L}_3) - \nu_1]\hat{n}_3 \cdot \vec{\delta}_{1,1} + [2\nu_3(1-\dot{L}_2) \\ & - \nu_1^*]\hat{n}_2 \cdot \vec{\delta}_{1,1}^* + [2\nu_3^*(1-\dot{L}_1) - \nu_2]\hat{n}_1 \cdot \vec{\delta}_{2,2} + [2\nu_1(1-\dot{L}_3) - \nu_2^*]\hat{n}_3 \cdot \vec{\delta}_{2,2}^* + [2\nu_1^*(1-\dot{L}_2) - \nu_3]\hat{n}_2 \cdot \vec{\delta}_{3,3} + [2\nu_2(1-\dot{L}_1) \\ & - \nu_3^*]\hat{n}_1 \cdot \vec{\delta}_{3,3}^* + [\nu_1 - \nu_2^*(1-\dot{L}_3)]\hat{n}_3 \cdot \vec{\Delta}_{1,1} + [\nu_1^* - \nu_3(1-\dot{L}_2)]\hat{n}_2 \cdot \vec{\Delta}_{1,1}^* + [\nu_2 - \nu_3^*(1-\dot{L}_1)]\hat{n}_1 \cdot \vec{\Delta}_{2,2} + [\nu_2^* - \nu_1(1 \\ & - \dot{L}_3)]\hat{n}_3 \cdot \vec{\Delta}_{2,2}^* + [\nu_3 - \nu_1^*(1-\dot{L}_2)]\hat{n}_2 \cdot \vec{\Delta}_{3,3} + [\nu_3^* - \nu_2(1-\dot{L}_1)]\hat{n}_1 \cdot \vec{\Delta}_{3,3}^* . \end{aligned} \tag{13}$$

Figures 3(a) and 3(b) illustrate the transfer functions of the optical bench and USO noises to the unequal arm interferometer data combination X_q (frequency and phase spectra, respectively). We have used in Eq. (9) worst-case laser center frequency differences ($\sim$300 MHz) and Doppler shifts ($\sim$15 MHz) [5]. For reference, the combined spectrum of proof-mass and optical path noises—the desired ultimate noise contributors for LISA—is shown. Unlike the situation [4] of equal laser center frequencies and constant armlengths, the optical bench noise now no longer cancels exactly. However, the expected [11] raw optical bench noise (10 nm/$\sqrt{\mathrm{Hz}}$) is still cancelled so well that it is negligibly

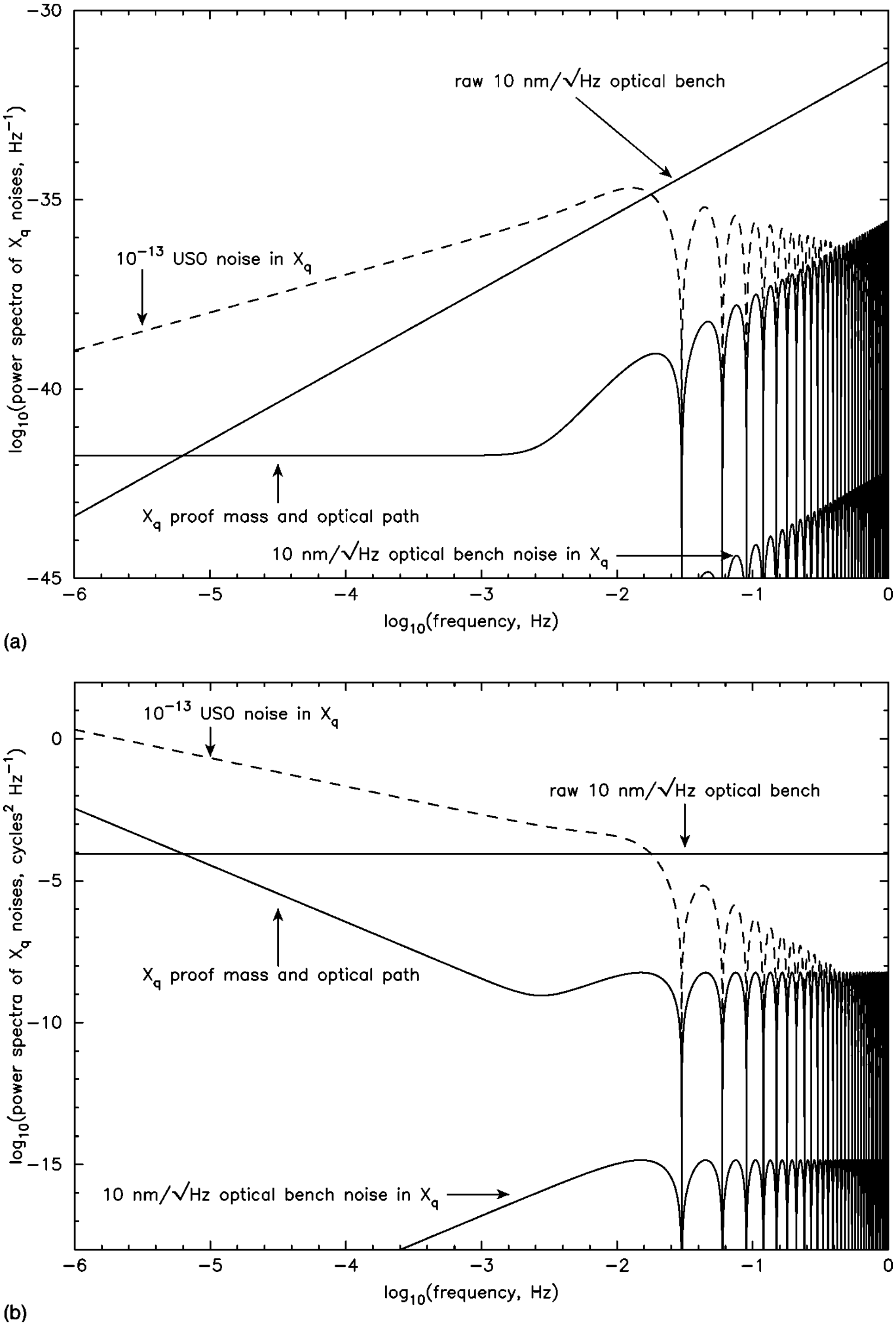

FIG. 3. (a) Noise spectrum, expressed as spectral density of fractional Doppler frequency fluctuations [3] versus Fourier frequency, for the unequal-arm Michelson interferometer combination X_q [Eq. (9)]. The curve labeled "X_q proof mass and optical path" is proof-mass acceleration noise (3×10^{-15} m sec^{-2} Hz$^{-1/2}$), and aggregate optical path noise (20×10^{-12} m Hz$^{-1/2}$) from Ref. [1]. They are also appropriately converted to fractional frequency fluctuations [4], and passed through their transfer functions to the X_q observable. This is the desired aggregate noise performance of the LISA Michelson interferometer data combination. The specified raw optical bench noise (10 nm Hz$^{-1/2}$) [11], and the optical bench noise after passing through the X_q transfer function are indicated by the other two solid lines. The dashed line shows the contribution to the X_q noise budget of an *uncancelled* state-of-the-art USO. Section IV of this paper shows how this noise can be removed to below that of the proof mass and the shot noise; (b) is as (a), but now the spectra are expressed in units of cycles squared, rather than fractional Doppler frequency noise.

below the optical path noise in the X_q observable.

The USO noise is, however, a problem. Shown in Figs. 3(a), 3(b) are the frequency and phase noise spectra of a state-of-the-art flight-qualified USO for the X_q observable. To make USO noise negligible compared with proof-mass-plus-optical-path noises would, for the X_q data combination, require about a three order of magnitude improvement in USO Allan deviation at integration times of about 1000 sec.

Figures 4(a) and 4(b) illustrate similarly for the symmetric Sagnac data combination ζ_q [Eq. (13)]. As with X_q, the expected bench noise does not cancel exactly but is nonetheless well below the optical path noise for the worst case center frequency differences and Doppler shifts. The USO noise situation in ζ_q is, however, even worse than it is in X_q. At midband ($\sim10^{-3}$ Hz), USO Allan deviation would have to be about four orders of magnitude better than the current state-of-the-art to be below the proof-mass-plus-optical-path noises.

It is unfortunate that such large improvements in USO performance seem required to make USO noise small enough to neglect, at least in the worst case of laser frequency offset and Doppler drifts. In the next section we de-

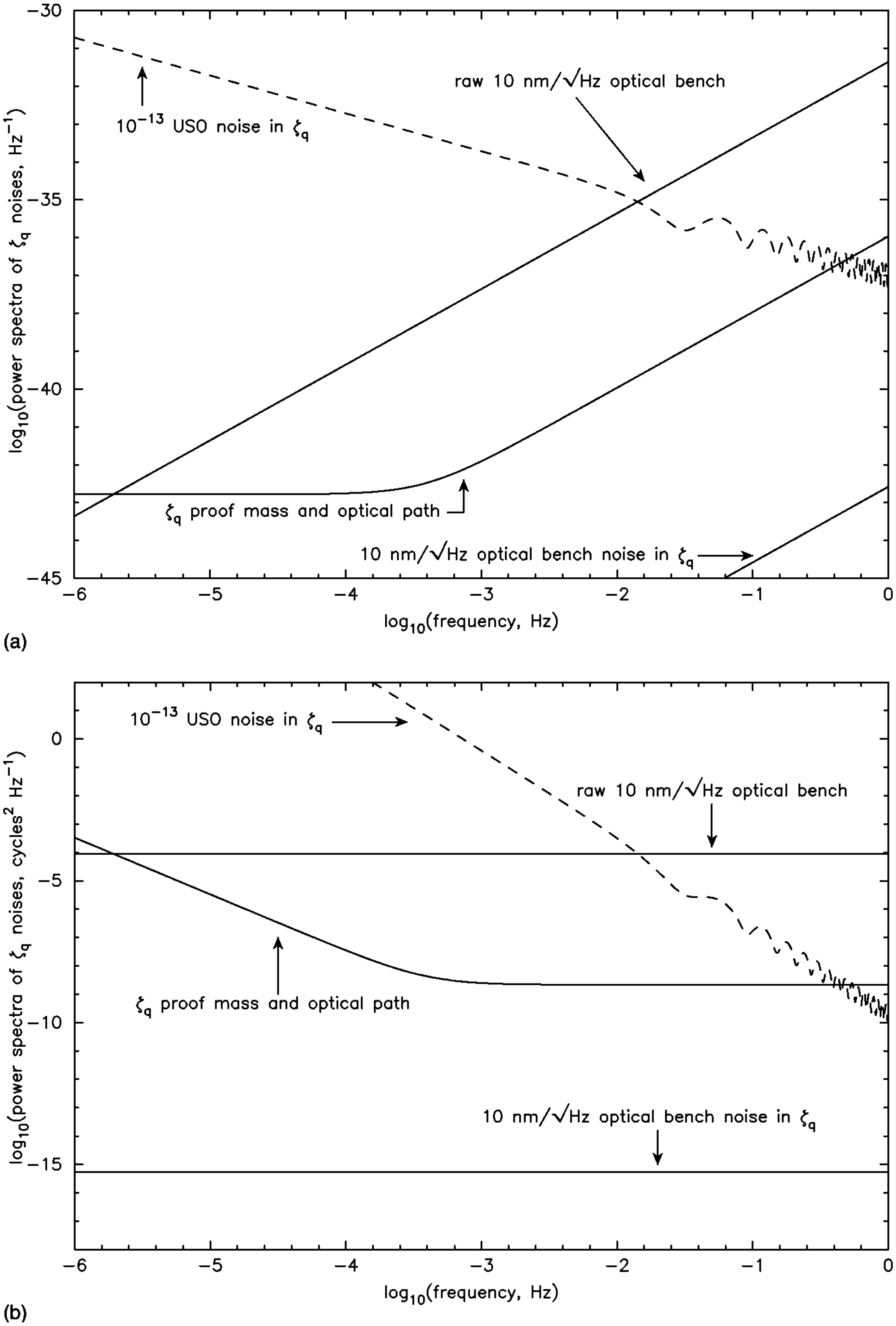

FIG. 4. As for Figs. 3(a) and 3(b), but for the laser-phase-noise cancelling data combination ζ_q [Eq. (13)].

rive procedures which show how the data can be corrected for the USO noise. The penalty for making these needed corrections, however, is an increase in the complexity of the LISA system.

IV. USO NOISE CORRECTION DATA

In the scheme first proposed by Bender *et al.* [1], in addition to the six main laser beams of frequencies ν_i, ν_i^* ($i=1,2,3$) which are transmitted between spacecraft, a second laser signal is superimposed on each beam by either modulating it at the frequency f_i of the onboard USO (creating two side bands), or more elegantly [6] combining each beam with a coherent second signal at $\nu_i + f_i$ or $\nu_i^* + f_i$, depending on the link considered. The main carrier signal, and a side band (of intensity perhaps ten times lower than the intensity in the carrier [1]) are transmitted , and at the receiving spacecraft they are heterodyned at a photodetector with a laser beam also containing a carrier and a side band (see Fig. 5). If the frequencies of the USOs are carefully selected to be a factor of about 3 to 10 larger than the laser frequency offsets (but to differ from each other by a few kilohertz) then the

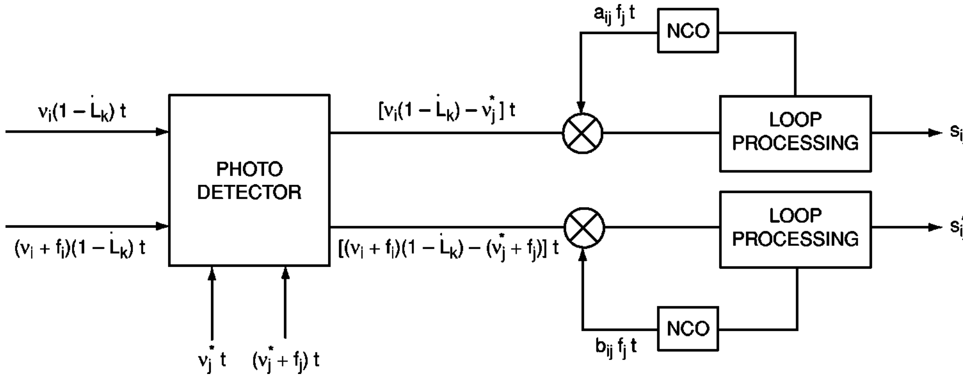

FIG. 5. Schematic diagram of the signal flow in the USO noise correction scheme. In addition to the six main laser beams of frequencies ν_i, ν_i^* $(i=1,2,3)$ which are transmitted between spacecraft, a second laser signal is superimposed on each beam by modulating it at the frequency f_i of the onboard USO, and generating a coherent second signal at ν_i+f_i or $\nu_i^*+f_i$, depending on the link considered. The main carrier signal, and a side band are transmitted, and at the receiving spacecraft they are heterodyned at a photodetector with a laser beam also containing a carrier and a side band. By properly selecting the frequencies of the USOs the lowest two phase differences can be distinguished and measured at the photodetector within its operational bandwidth. These two phase differences are given by the difference between the phases of the two carriers, and the difference of the phases of the two side bands, respectively. They are then independently down converted with coefficients a_{ij} and b_{ij}. This process provides six additional data records, s'_{ij}, which are sufficient for USO noise correction (see Sec. IV for details).

lowest two phase differences can be distinguished and measured at the photodetector within its operational bandwidth. These two phase differences are given by the difference between the phases of the two carriers, and the difference of the phases of the two side bands, respectively. They are then independently down converted with coefficients a_{ij} and b_{ij} (with b_{ij} *different* from a_{ij}, contrary to what was envisaged in Ref. [7]). This process provides six additional data records we will call s'_{ij} (see Fig. 5). (We will see that this data suffices for USO noise correction—no modulation data need be taken between lasers on the same spacecraft, even if their frequencies are offset and bring in further noise terms.) Consider, for instance, the phase difference between the second signal transmitted by bench 3 and the second at the receiving bench 1*

$$\begin{aligned} s'_{21} = {} & [(\nu_3+f_3)(1-\dot{L}_2)-\nu_1^*-f_1-b_{21}f_1]t+p_{3,2}+q_{3,2}-p_1^* \\ & -q_1-b_{21}q_1-\nu_3\hat{n}_2\cdot\vec{\Delta}_{3,2}+\nu_3(1-\dot{L}_2)[2\hat{n}_2\cdot\vec{\delta}_1^* \\ & -\hat{n}_2\cdot\vec{\Delta}_1^*]+s_{21}^{\mathrm{gw}}+s_{21}'^{\,\mathrm{opt.\ path}}, \end{aligned} \tag{14}$$

where any differences in the gravitational wave signals, the proof mass and the bench noise, from those given in Eq. (1) for s_{21}, have not been included since they are negligible as a consequence of the condition $f_i \ll \nu_i$. Note that the numerical coefficient b_{21}, determined by the following equation:

$$b_{21}=\frac{(\nu_3+f_3)(1-\dot{L}_2)-(\nu_1^*+f_1)}{f_1}, \tag{15}$$

is distinct from a_{21} given by Eq. (5) (although they will be close if all the f_i are close).

Following Hellings [7], where a three-spacecraft, three-laser configuration was treated, let us now introduce the quantities $r_{21}\equiv(s_{21}-s'_{21})/f_3$ and similarly $r_{31}\equiv(s_{31}-s'_{31})/f_2$ (and cyclic permutations of their indices). By taking into account Eqs. (1)–(7) we derive the following expressions for r_{21} and r_{31}:

$$r_{21}=(1-\dot{L}_2)\frac{q_1}{f_1}-\frac{q_{3,2}}{f_3}+\frac{[s_{21}^{\mathrm{opt.\ path}}-s_{21}'^{\,*\mathrm{opt.\ path}}]}{f_3}, \tag{16}$$

$$r_{31}=(1-\dot{L}_3)\frac{q_1}{f_1}-\frac{q_{2,3}}{f_2}+\frac{[s_{31}^{\mathrm{opt.\ path}}-s_{31}'^{\,\mathrm{opt.\ path}}]}{f_2}. \tag{17}$$

The r_{ij} are six additional data streams that LISA must take when USO noise is to be eliminated. By neglecting terms proportional to $\dot{L}_i$, Eqs. (16), (17) can be rewritten to sufficient accuracy as follows:

$$r_{21}=\frac{q_1}{f_1}-\frac{q_{3,2}}{f_3}+\frac{[s_{21}^{\mathrm{opt.\ path}}-s_{21}'^{\,\mathrm{opt.\ path}}]}{f_3}, \tag{18}$$

$$r_{31}=\frac{q_1}{f_1}-\frac{q_{2,3}}{f_2}+\frac{[s_{31}^{\mathrm{opt.\ path}}-s_{31}'^{\,\mathrm{opt.\ path}}]}{f_2}, \tag{19}$$

with the remaining expressions obtained by cyclic permutations of the indices. Since we have only three USO noises q_i, and six calibration data r_{ij}, $i,j=1,2,3$, $i\neq j$, there are relationships among the six r_{ij} data. They are given by the following expressions:

$$K_1\equiv r_{23,13}+r_{12,3}+r_{31}-r_{32,12}-r_{13,2}-r_{21}=0, \tag{20}$$

with two more identities obtained by permutation of the indices in Eq. (20), while the fourth identity is

$$K_0\equiv r_{12,2}-r_{21,1}+r_{23,3}-r_{32,2}+r_{31,1}-r_{13,3}=0, \tag{21}$$

which is consistent with the first three, in fact,

$$K_0-K_{0,123}=K_{1,1}-K_{1,23}+K_{2,2}-K_{2,31}+K_{3,3}-K_{3,12}. \tag{22}$$

In what follows we will show how to use the additional data r_{ij} in order to remove the USO noise from the laser-noise-free combinations presented in the previous section.

In order to remove from X_q the USO phase fluctuations, one must find appropriate time-delay combinations of the r_{ij} $(i,j=1,2,3)$ data that provide the combinations of the USO phase noises that occur in Eq. (9). After taking into account the expressions for the r_{ij} determined by Eqs. (18), (19), it is easy to find the following identities:

$$[q_1-q_{1,22}]=f_1[r_{21}+r_{23,2}], \tag{23}$$

$$[q_1-q_{1,33}]=f_1[r_{31}+r_{32,3}], \tag{24}$$

$$[q_{3,2}-q_{3,233}]=f_3[r_{21,33}-r_{21}+r_{31}+r_{32,3}], \tag{25}$$

$$[q_{2,3}-q_{2,322}]=f_2[r_{31,22}-r_{31}+r_{21}+r_{23,2}]. \tag{26}$$

In Eqs. (23)–(26) we have disregarded the optical path noise terms because the magnitude of the coefficients a_{ij} and c_{ij} $(i,j=1,2,3;i\neq j)$ is smaller than unity (perhaps as small as 0.1), as a consequence of the values of the USO frequencies made earlier when we discussed the heterodyne measurement. Substituting Eqs. (23)–(26) into Eq. (9) we finally find the corrected response X, defined to be

$$\begin{aligned}X\equiv X_q&-a_{32}f_2[r_{31,22}-r_{31}+r_{21}+r_{23,2}]+a_{23}f_3[r_{21,33}-r_{21}\\&+r_{31}+r_{32,3}]-a_{31}f_1[r_{21}+r_{23,2}]+a_{21}f_1[r_{31}+r_{32,3}]\\&+\frac{1}{2}c_{21}f_1[r_{23,233}+r_{21,33}-r_{23,2}-r_{21}+r_{32,223}+r_{31,22}\\&-r_{32,3}-r_{31}].\end{aligned} \tag{27}$$

Since the unequal-arm interferometric response X is antisymmetric with respect to permutation of the indices (2,3), the corresponding combinations used for calibrating out the USO noise from X_q have been antisymmetrized by using the identities given by Eqs. (20), (21). The other two unequal-arm interferometer responses, which we denote Y and Z, follow from Eq. (27) after performing a cyclic permutation of the spacecraft indices.

In the case of the α_q combination, it is impossible to calibrate out exactly the USO noise using the combinations r_{ij} [7]. However, we can rewrite the USO phase noises in terms of some of the r_{ij} data and only the USO phase noise q_1 by using the following additional identities:

$$\begin{aligned}q_{1,123}&=q_1-f_1[r_{23,13}+r_{12,3}+r_{31}],\\&=q_1-f_1[r_{32,12}+r_{13,2}+r_{21}],\end{aligned} \tag{28}$$

$$q_{2,12}=\frac{f_2}{f_1}q_1-f_2[r_{21}+r_{13,2}], \tag{29}$$

$$q_{3,13}=\frac{f_3}{f_1}q_1-f_3[r_{31}+r_{12,3}]. \tag{30}$$

The USO noise terms involving the q_i in Eq. (11) then become

$$\begin{aligned}&[(a_{31}-a_{21}+2c_{21})f_1+(a_{12}-a_{32}+2c_{32})f_2+(a_{23}-a_{13}\\&+2c_{13})f_3]\frac{q_1}{f_1}-f_1c_{21}[r_{23,13}+r_{31}+r_{12,3}]-f_2[c_{32}\\&+a_{12}]r_{31}-f_3[c_{13}-a_{13}]r_{21}-f_2[c_{32}-a_{32}][r_{21}+r_{13,2}]\\&-f_3[c_{13}+a_{23}][r_{31}+r_{12,3}].\end{aligned} \tag{31}$$

If we now take into account the expressions for the coefficients a_{ij} and c_{ij}, the first term in Eq. (31) becomes

$$[(\nu_2-\nu_3^*)\dot{L}_1+(\nu_3-\nu_1^*)\dot{L}_2+(\nu_1-\nu_2^*)\dot{L}_3]\frac{q_1}{f_1}. \tag{32}$$

This corresponds to relative frequency fluctuations (or strain noise) of the order of about 10^{-27} under the assumptions of having laser frequency offsets of a few hundred megahertz, a laser center frequency equal to 3×10^{14} Hz, Doppler term $\dot{L}_i$ equal to about 5×10^{-8} [5], and a USO frequency stability of about 10^{-13}. Thus we can ignore it and, after some algebra, define the laser-noise-free and USO-noise-free reduced data α to be

$$\begin{aligned}\alpha\equiv\alpha_q&+\left[\frac{1}{2}f_1c_{21}+f_2c_{32}+f_3c_{13}+f_2a_{12}+f_3a_{23}\right]r_{31}\\&-\left[\frac{1}{2}f_1c_{31}+f_3c_{23}+f_2c_{12}+f_3a_{13}+f_2a_{32}\right]r_{21}+\left[f_2c_{32}\right.\\&\left.+\frac{1}{2}f_1c_{21}-f_2a_{32}\right]r_{13,2}-\left[f_3c_{23}+\frac{1}{2}f_1c_{31}-f_3a_{23}\right]r_{12,3}\\&+\frac{1}{2}f_1c_{21}r_{23,13}-\frac{1}{2}f_1c_{31}r_{32,12}\end{aligned} \tag{33}$$

with α_q given by Eq. (11). Similar to the unequal-arm interferometric response X, also α should be antisymmetric with respect to permutation of the indices (2,3). The combinations in Eq. (31) used for calibrating out the USO noise from α_q have therefore, in Eq. (33), been antisymmetrized by using the identities given by Eqs. (20), (21). The remaining two responses that we will denote β and γ follow from Eq. (33) after performing cyclic permutation of the spacecraft indices.

As for the α_q combination, also for the symmetric Sagnac combination ζ_q it is impossible to calibrate the USO noise out exactly by using the r_{ij} [7]. However, if we rewrite the USO phase noises in terms of some of the r_{ij} and the USO phase noise $q_{1,1}$ by using the following identities:

$$q_{1,23}=q_{1,1}+f_1[r_{12,2}-r_{21,1}-r_{32,2}], \tag{34}$$

$$q_{3,12}=\frac{f_3}{f_1}q_{1,1}-f_3r_{21,1}, \tag{35}$$

$$q_{2,13}=\frac{f_2}{f_1}q_{1,1}-f_2r_{31,1}, \tag{36}$$

$$q_{2,2}=\frac{f_2}{f_1}\ q_{1,1}+f_2[r_{12,2}-r_{21,1}], \tag{37}$$

$$q_{3,3}=\frac{f_3}{f_1}q_{1,1}+f_3[r_{13,3}-r_{31,1}], \tag{38}$$

the USO noise terms involving the q_i in Eq. (13) become

$$\begin{aligned}&[(a_{31}-a_{21}+2c_{21})f_1+(a_{12}-a_{32}+2c_{32})f_2+(a_{23}-a_{13}\\&\quad+2c_{13})f_3]\frac{q_{1,1}}{f_1}+f_2(a_{12}-a_{32}+c_{32})[r_{12,2}-r_{21,1}]\\&\quad+f_3(a_{23}-a_{13}+c_{13})[r_{13,3}-r_{31,1}]+f_1c_{21}[r_{12,2}-r_{21,1}\\&\quad-r_{32,2}]-f_2c_{32}r_{31,1}-f_3c_{13}r_{21,1}\,. \end{aligned}\tag{39}$$

Notably, the coefficient of the USO noise $q_{1,1}$ given in Eq. (39) is identical to that in the corresponding term in Eq. (31), making again the contribution from this remaining USO noise negligible. Thus we define the laser-noise-free and USO-noise-free reduced data ζ to be

$$\begin{aligned}\zeta&\equiv\zeta_q+\frac{1}{3}f_1(a_{31}-a_{21})[r_{13,3}-r_{31,1}+r_{12,2}-r_{21,1}]+\frac{1}{3}f_2(a_{12}\\&\quad-a_{32})[r_{21,1}-r_{12,2}+r_{23,3}-r_{32,2}]+\frac{1}{3}f_3(a_{23}-a_{13})[r_{32,2}\\&\quad-r_{23,3}+r_{31,1}-r_{13,3}]+\frac{1}{6}f_1c_{21}[3r_{32,2}+3r_{23,3}-r_{31,1}\\&\quad+r_{13,3}-r_{21,1}+r_{12,2}]+\frac{1}{6}f_2c_{32}[3r_{13,3}+3r_{31,1}-r_{12,2}\\&\quad+r_{21,1}-r_{32,2}+r_{23,3}]+\frac{1}{6}f_3c_{13}[3r_{21,1}+3r_{12,2}-r_{23,3}\\&\quad+r_{32,2}-r_{13,3}+r_{31,1}]\end{aligned}\tag{40}$$

with ζ_q given by Eq. (13). Note that expression given in Eq. (40) for calibrating the USO noises has been made antisymmetric under permutation of any pair of the three indices, consistently with the symmetry properties of the laser-noise-free combination ζ.

V. SUMMARY AND CONCLUSIONS

We have treated a fairly general model of the LISA detector with unequal, time-dependent arm lengths, six lasers with center frequencies different from each other, six optical benches, six proof masses, and three USOs. These oscillators—along with their noises—had to be introduced to remove the large beat notes due to laser center frequency offsets and Doppler shifts caused by armlength changes.

We generalized our previous time-delay interferometry (unequal arm Michelson interferometer X, α, symmetric Sagnac ζ, etc.) results, presenting here data combinations which again cancel the leading noise (laser phase fluctuations) and preserve gravitational waves, but which are now more complex. These generalized data combinations imply transfer functions of the noises to the time-delay-interferometry observables; they thus provide a framework within which noise-budget trade-offs (USO performance versus arm-length changes due to orbits versus center frequency differences between the lasers) can be made.

With present specifications, phase noise from noninertial motions of the optical benches will be negligible. We give spectra of remaining frequency and phase noises in the laser-noise-free data combinations X and ζ. For current-generation USO performance, however, the added USO noise is unacceptably high and thus must be calibrated. We generalized, for the realistic LISA configuration, previous ideas about how to calibrate and remove USO noise to acceptable levels. This calibration scheme is described in detail in Sec. IV. We conclude that the time-delay-interferometry results generalize to this realistic model of LISA, but now eighteen data streams have to be taken. This allows us to calibrate out the USO noises from the data, with the noise budget reduced to that of the proof-mass and laser shot noises.

In order to minimize the number of data streams for synthesizing interferometers with the LISA three-spacecraft, it has been proposed to have very small frequency offsets by phase locking the lasers to one master laser. One then performs sets of two-way measurements [1] and constructs the unequal-arm Michelson interferometric responses [1,2], although the other useful data combinations are lost. While major laser frequency offsets are now avoided, onboard oscillators for removing the Doppler-induced beat notes are still needed. The transfer functions of the USO noises into the interferometric responses are now different from those obtained using one-way measurements as discussed in this paper, and furthermore additional one-way measurements (such as the s'_{ij} introduced in this paper) for calibrating the USOs noises are no longer available. Since the technique for removing USO noises presented in this paper is based on one-way measurements, further work is needed in order to identify a USO noise calibration technique when two-way coherent measurements are used instead.

ACKNOWLEDGMENTS

We thank Dr. Lute Maleki for valuable discussions regarding USOs and space-qualified frequency standards. This research was performed at the Jet Propulsion Laboratory, California Institute of Technology, under contract with the National Aeronautics and Space Administration.

APPENDIX: TIME-DELAY INTERFEROMETRY USING DOPPLER DATA

The body of this paper on interferometry with separately moving spacecraft, communicating with offset laser beams, has been presented in terms of measured phases, using notation close to that of Refs. [6,7] to facilitate comparison of results. The use of phase variables in conventional interferometry is customary, as phase change is seen as a direct result of displacement of proof masses $\Delta L/\lambda$. In our previous papers on time-delay analysis [2–4] we maintained a consistent notation using frequency variables; varying inter-

TABLE I. Glossary of symbols representing phase observables introduced in this article, and relationships to their corresponding frequency observables [4].

ν_0	Averaged or nominal frequency of LISA's optical lasers. Used to normalize frequency variations to be nondimensional.
ν_i , ν_i^*	Laser center frequencies.
s_{ij} (t)	Measured time series of phase difference between received laser beam from distant spacecraft and local laser; time integral of ν_0 y_{ij} (t) as given in Refs. [3] and [4].
τ_{ij} (t)	Measured time series of phase difference between lasers on adjacent optical benches within a given spacecraft; time integral of ν_0 z_{ij} (t) as defined in Ref. [4].
$\vec{\Delta}_i$ $\vec{\Delta}_i^*$ (t)	Random displacement vectors of the optical benches; time integrals of V_i (t), V_i^* (t), respectively, as given in Ref. [4].
$\vec{\delta}_i$ (t), $\vec{\delta}_i^*$ (t)	Random displacement vectors of the proof masses; time integral of $\vec{\nu}_i$ (t), $\vec{\nu}_i^*$ (t), respectively, as given in Ref. [4].
μ_i (t)	Phase variation in optical fiber connecting adjacement optical benches; time integral of $\nu_0\,\eta_i$ (t) in Ref. [4].
f_i	USO center frequencies.
q_i (t)	Random phase fluctuations of the USOs.
Q_i (t)	$\frac{\dot{q}_i(t)}{f_i}=$ fractional frequency fluctuations of the USOs.
p_i (t), p_i^* (t)	Random phase fluctuations of the lasers; time integrals of $\nu_i C_i(t)$, $\nu_i^* C_i^*(t)$ in Ref. [4], respectively.
$\dot{L}_i$	Arm length variations/c; expected maximum for LISA is approximately 5×10^{-8}.
$s'_{ij}(t)$	Measured time series of phase difference between Doppler shifted laser calibration signal from a remote spacecraft, and the local laser signal offset by the local USO frequency [Eq. (14) and Fig. 5].
a_{ij}	Coefficient used to remove large frequency offset between signal from distant spacecraft and the local laser; used in the measurement of $s_{ij}(t)$ [Eqs. (5), (6) and Fig. 5].
b_{ij}	Coefficient used to remove large frequency offset between the laser calibration signal from a remote spacecraft and the local laser signal offset by the local USO frequency; used in the measurement of $s'_{ij}(t)$ [Eqs. (14), (15) and Fig. 5].
c_{ij}	Difference in frequencies of lasers on adjacent optical benches divided by USO frequency for that spacecraft; used in the measurement of $\tau_{ij}(t)$ [Eq. (7)].
$r_{ij}(t)$	Difference between $s_{ij}(t)$ and $s'_{ij}(t)$ time series, divided by the USO frequency [see Sec. IV, Eqs. (16), (17) ff].
ω_{ij}	Difference between Doppler shifted frequency of remote laser and frequency of local laser [Eq. (A2) and Eqs. (5), (6)].
σ_{ij}	Difference between frequencies of lasers on adjacent optical benches [Eq. (A6), and Eq. (7)].

ference phenomena then are understood as arising from Doppler shifts upon reflection from moving onboard components such as mirrors, proof masses, and optical benches $\Delta\nu/\nu_0 = \dot{L}$. The two alternatives of course yield identical results.

We have been inclined to prefer the frequency description because the wave form of the propagating Riemann curvature (spin-2 radiation) that constitutes a gravitational wave train appears directly as a fractional frequency modulation—a time-dependent Doppler shift—imposed on an observed light beam [3,9,10]. This formulation has always been used in gravitational wave search experiments using microwave tracking of spacecraft. The gravitational wave effect on a phase variable, on the other hand, is the time integral of the amplitude of the gravitational wave train. But of course observational time series data can be differentiated. And to further confuse the issue it may well be said that experimental measurement of time-dependent frequency shifts itself come down to counting the phase at precisely spaced time intervals.

In the following we give equivalent frequency variable formulations of the key equations used in this paper, to facilitate comparison with, and in the notation of, Refs. [2–4]. In Table I we provide a conversion glossary between the two notations; the only remaining source of any confusion might be that we do not change notation for the laser-noise-free data combinations themselves. For X, Y, Z, α, β, γ, ζ, whether phase or frequency data is described will have to be determined from the context.

We now will write an equation, equivalent to Eq. (3) above, for the fractional frequency variation $y_{31}\equiv\dot{s}_{31}/\nu_0$ measured on the left bench of spacecraft 1. The phase rate is made dimensionless with a conventional—or perhaps averaged—laser frequency ν_0. This equation describes the mixing of a laser beam from the right bench of spacecraft 2, emitted with frequency ν_2^* $(1+C_2^*)$, time delayed and Doppler shifted on transmission along L_3 to spacecraft 1, and inertially referenced before mixing with the local laser light of frequency ν_1 $(1+C_1)$. C_2^*, C_1, etc., are the time-dependent fractional frequency variations of the lasers, as in Eqs. (2.1)–(2.4) of Ref. [4]. The Doppler shifts will involve $\dot{L}_3$ and $\vec{V}_2$, $\vec{V}_1$, $\vec{v}_2$, $\vec{v}_1$, the fluctuating velocities of the benches and proof masses with respect to the inertial frame of spacecraft 2 and 1, respectively. So $\vec{V}_2^* = \dot{\vec{\Delta}}_2^*$, $\vec{v}_1^* = \dot{\vec{\delta}}_1^*$, etc. The output after mixing at a photodiode is a $\sim 10^8$ Hz beat frequency that is tracked—or down converted—with a locally generated frequency we will denote as $\omega_{31}(1+Q_1)$. ω_{31} is slowly varying with the LISA geometry, while $Q_1(t)$ is the fractional frequency fluctuation introduced by the USO (or other frequency standard) on spacecraft 1. In the body of this paper we took $\omega_{31} = a_{31} f_1$, the fractional fluctuations were $Q_1 = \dot{q}_1 / f_1$, and $C_1 = \dot{p}_1 / \nu_1 \simeq \dot{p}_1 / \nu_0$. Thus we write in terms of frequency shifts

$$\nu_0 y_{31} = \nu_2^* [1 + C_{2,3}^* + \vec{n}_3 \cdot \vec{V}_{2,3}^*][1 - \dot{L}_3][1 + \vec{n}_3 \cdot \vec{V}_1 - 2\vec{n}_3 \cdot \vec{v}_1] - \nu_1(1 + C_1) - \omega_{31}(1 + Q_1) + \nu_0 y_{31}^{gw} + \nu_0 y_{31}^{\text{opt. path}}. \tag{A1}$$

We now impose the frequency tracking condition on the slowly time varying terms, finding

$$\omega_{31} = \nu_2^*(1 - \dot{L}_3) - \nu_1, \tag{A2}$$

and the fluctuations y_{31} become

$$\nu_0 y_{31} = \nu_2^*(1 - \dot{L}_3) C_{2,3}^* + \nu_2^*(1 - \dot{L}_3)\vec{n}_3 \cdot \vec{V}_{2,3}^* + \nu_2^*(1 - \dot{L}_3) \times [\vec{n}_3 \cdot \vec{V}_1 - 2\vec{n}_3 \cdot \vec{v}_1] - \nu_1 C_1 - \omega_{31} Q_1 + \nu_0 y_{31}^{gw} + \nu_0 y_{31}^{\text{opt. path}}, \tag{A3}$$

which is a direct generalization of Eq. (2.3) of Ref. [4]. Similarly for other frequency readouts we will have for Eq. (2.1) of Ref. [4]

$$\omega_{21} = \nu_3(1 - \dot{L}_2) - \nu_1^*, \tag{A4}$$

$$\nu_0 y_{21} = \nu_3(1 - \dot{L}_2) C_{3,2} - \nu_3(1 - \dot{L}_2)\vec{n}_2 \cdot \vec{V}_{3,2} + \nu_3(1 - \dot{L}_2)[2\vec{n}_2 \cdot \vec{v}_1^* - \vec{n}_2 \cdot \vec{V}_1^*] - \nu_1^* C_1^* - \omega_{21} Q_1 + \nu_0 y_{21}^{gw} + \nu_0 y_{21}^{\text{opt. path}}, \tag{A5}$$

and cyclic permutations.

Laser frequency comparison data between adjacent optical benches were denoted z_{ij} in Ref. [4]. Evidently $\nu_0 z_{ij} = \dot{\tau}_{ij}$, and with the following synthesized frequencies used for the down conversion

$$\sigma_{31} \equiv \nu_1^* - \nu_1 = f_1 c_{31} = -\sigma_{21}, \tag{A6}$$

we have generalizations of Eqs. (2.2) and (2.4) of Ref. [4]

$$\nu_0 z_{21} = \nu_1 C_1 + 2\nu_1 \vec{n}_3 \cdot (\vec{v}_1 - \vec{V}_1) + \nu_1 \eta_1 - \sigma_{21} Q_1 - \nu_1^* C_1^*, \tag{A7}$$

$$\nu_0 z_{31} = \nu_1^* C_1^* - 2\nu_1^* \vec{n}_2 \cdot (\vec{v}_1^* - \vec{V}_1^*) + \nu_1^* \eta_1 - \sigma_{31} Q_1 - \nu_1 C_1. \tag{A8}$$

Any frequency shifts due to the optical fibers result from their varying phase rates

$$\nu_1 \eta_1 \simeq \nu_1^* \eta_1 \simeq \dot{\mu}_1. \tag{A9}$$

When Eqs. (A3), (A5), (A7), and (A8) are used to find laser-noise-free frequency data combinations, it becomes clear that delayed terms must also be multiplied by corresponding Doppler factors [e.g., $y_{ij,k}$ by $(1 - \dot{L}_k)$, etc.]. In all the already derived combinations of frequency data, the comma can simply be redefined, or, better for emphasis, be replaced by a semicolon. A semicolon subscripted index i is now understood to mean not only time delay by L_i but also multiplication by the Doppler factor $(1 - \dot{L}_i)$. This generalized result can, of course, also be obtained directly by time differentiation of the laser-noise-free phase combinations given in the main body of the paper, being careful to correctly use the chain rule on functions of delayed times. As a single example, the USO and optical bench frequency noises in the unequal-arm interferometer combination $\nu_0 X_q$ are, respectively, equal to

$$\omega_{32}(Q_{2;3} - Q_{2;223}) - \omega_{23}(Q_{3;2} - Q_{3;233}) + \omega_{31}(Q_1 - Q_{1;22}) - \omega_{21}(Q_1 - Q_{1;33}) + \sigma_{21}(Q_{1;2233} - Q_{1;33} - Q_{1;22} + Q_1), \tag{A10}$$

$$\omega_{31}(\vec{n}_3 \cdot \vec{V}_{1;22} - \vec{n}_3 \cdot \vec{V}_1) + \omega_{21}(\vec{n}_2 \cdot \vec{V}^*{}_{1;33} - \vec{n}_2 \cdot \vec{V}^*{}_1) - \omega_{32}(\vec{n}_3 \cdot \vec{V}^*{}_{2;223} - \vec{n}_3 \cdot \vec{V}^*{}_{2;3}) - \omega_{23}(\vec{n}_2 \cdot \vec{V}_{3;233} - \vec{n}_2 \cdot \vec{V}_{3;2}). \tag{A11}$$

[1] P. Bender, K. Danzmann, and the LISA Study Team, Laser Interferometer Space Antenna for the Detection of Gravitational Waves, Pre-Phase A Report No. MPQ233, Max-Planck-Institüt für Quantenoptik, Garching, 1998.
[2] M. Tinto and J.W. Armstrong, Phys. Rev. D **59**, 102003 (1999).
[3] J.W. Armstrong, F.B. Estabrook, and M. Tinto, Astrophys. J. **527**, 814 (1999).
[4] F.B. Estabrook, M. Tinto, and J.W. Armstrong, Phys. Rev. D **62**, 042002 (2000).
[5] W.M. Folkner, F. Hechler, T.H. Sweetser, M.A. Vincent, and P.L. Bender, Class. Quantum Grav. **14**, 1543 (1997).
[6] R.W. Hellings, G. Giampieri, L. Maleki, M. Tinto, K. Danzmann, J. Homes, and D. Robertson, Opt. Commun. **124**, 313 (1996).
[7] R.W. Hellings, Phys. Rev. D **64**, 022002 (2001).
[8] J. Gowar, *Optical Communication Systems* (Prentice/Hall International, 1984), pp. 136–140.
[9] H.D. Wahlquist, Gen. Relativ. Gravit. **19**, 1101 (1987).
[10] M. Tinto, Phys. Rev. D **53**, 5354 (1996).
[11] W.M. Folkner (private communication).
[12] M. Peterseim, D.I. Robertson, K. Danzmann, H. Welling, and P. Bender, Adv. Space Res. **25**, 1143 (2000).